ANANet - MAASNet: A Dual-Stage Framework for Image Tampering Detection and Localization

MR. PRINCE JOY[1], DR. B. JAYANTHI[2]

[1]*Research Scholar, Department of Computer Science RVS College Sulur. Coimbatore,*
E-Mail:- princejpalat@gmail.com
[2]*Associate Professor, Department of Computer Science, RVS College Sulur. Coimbatore,*
E-Mail:- jayanthi@rvsgroup.com

KEYWORDS

Adaptive Noise-Aware Neural Network, Multi-Layer Adaptive Attention Segmentation Network, Denoising, Segmentation, Image tampering.

ABSTRACT

Tampering localization and detection are increasingly indispensable steps with the increasing use of sophisticated manipulation techniques. Herein, we present a two-stage approach that involves Adaptive Noise-Aware Neural Network (ANANet) as preprocessing and Multi-Layer Adaptive Attention Segmentation Network (MAASNet) as segmentation for enhancing tampering detection from images. ANANet effectively removes noise without discarding informative image features so that the regions that have been tampered are not concealed at preprocessing. Following denoising, MAASNet uses multi-layer adaptive attention mechanisms for accurate segmentation of tampered regions and also improves the accuracy of tampering localization. The scheme has the ability to handle most types of image forgeries, i.e., copy-move, splicing, and in painting. The experimental outcome indicates that our scheme is superior to state-of-the-art schemes in terms of detection accuracy, noise variance resistance, and quality of segmentation and hence is an effective solution to image forensics issues.

I. Introduction

Computer vision and image processing are now essential research fields with uses spanning from medical imaging to security and multimedia forensics. These problems, including image noise, tampering, and forgery, have inspired the creation of sophisticated algorithms for image denoising, segmentation, and authentication. Researchers have explored new techniques to solve these problems using machine learning, deep learning, and optimization methods.

Image denoising is extremely important in image quality improvement, especially in medical imaging and hyperspectral image processing. Deep learning techniques such as generative adversarial networks (GANs), autoencoders, and clustering-based methods have been extensively explored [1], [2], [3]. Superpixel-based fuzzy clustering algorithms [4] and conditional GANs [5] have also worked well for denoising. Besides that, hybrid approaches like singular value decomposition in combination with adaptive clustering have been used to effectively suppress the noise [6]. Denoising of CT at low dose has also enticed weakly supervised learning where research has documented improvement using Wasserstein GANs and combination loss functions [7].

Segmentation is necessary to obtain significant information from images, especially medical and remote sensing images. Conventional techniques, including Otsu thresholding, have been enhanced with optimization techniques like fruit fly optimization [8] and Darwinian particle

swarm optimization [9]. Multimodal deep learning segmentation methods have also pushed the boundaries of the field, especially for medical imaging [10].

With the advent of digital media, the need for image forgery detection and watermarking methods has arisen to authenticate images. Recompression-based approaches of deep learning-based forgery detection include recompressing images to detect inconsistencies [11]. Fused feature extraction methods have also been utilized for detection and localization of tampering [12]. New developments in digital watermarking such as dual-matrix-based block mapping have enhanced image authentication with self-recovery [13]. Moreover, hyperchaotic encryption with watermarking has been suggested for copyright protection [14]. For Deepfake detection, active forensic methods with watermarking have emerged as useful countermeasures [15].

Unsupervised machine learning methods have been utilized to denoise scanning electron microscope (SEM) images in order to increase the quality of defect inspection [16]. Denoising hyperspectral images through Convolutional Neural Networks (CNNs) has also increased the quality of images in geoscience [17]. Deep learning methods have also been widely utilized for PET image denoising [18].

The first work by [19] is a hardware implementation description of an AI autoencoder for numerical image denoising. Its performance is contrasted in the paper with the conventional methods. The second work by [20] is regarding deep learning approaches to identify spoofed images with high accuracy using the ResNet model. The authors also propose a prototype system that is practical for real applications.

Contribution: This research enhances image processing by using more sophisticated deep learning and optimization methods. It enhances image denoising by using more efficient noise reduction algorithms, resulting in clearer images for medical and scientific application. It enhances image segmentation by using intelligent algorithms for detecting features more accurately. In image forgery detection, this research enhances security by developing better means of detecting alteration and inserting digital watermarks for security purposes. Overall, the study provides tangible solutions to enhancing image quality, security, and authenticity.

The paper has been organized for delivering a total review of the image processing innovation. Section 2 is related work survey explaining available methods for image denoising, image segmentation, forgery detection and their shortcoming. Section 3 presents methodology proposed in this work detailing used deep learning techniques, optimization process and digital watermarking involved therein. Section 4 explains experimental methodology, i.e., datasets used, measurement scales, and comparative results analysis with state-of-the-art schemes. Section 5 presents qualitative analysis in terms of implications and applications of the results. Lastly, Section 6 presents the concluding overview of major contributions and future research work areas. Such sequential systematic methodology ensures readability and reasonableness in exposition of the paper.

II. Background Study

Image tampering identification techniques include image denoising and segmentation for manipulation checking and visual integrity check. Wavelet transforms, compressive sensing and Deep Learning models are used to denoise removing the noise with the least loss in high frequency aspects. Segmented image is used to isolate manipulated regions by means of thresholding, active contour model, and deep neural network. Numerous studies have proved that it is a good way of analysis and digital content authentication in forensic. Regarding the improvements in both the area of machine learning and computer vision, accuracy level of the image tampering detection and prevention has been greatly improved.

Mahdaoui et al. (2022) [21] introduced an image denoising technique using a Compressive Sensing (CS) approach with regularization constraints (RCs). The method used those sparse image representations for image reconstruction based on noise. It had effectively preserved image structures and details as well as further optimized the noise reduction vs. signal fidelity trade-off. This work exceeded the results of all other conventional denoising techniques. The method delivered substantial utility during HQIR applications.

The authors of Mandisha et al. (2025) [22] conducted forensic research on digital images through WT according to the following description. They carried out their research regarding site of tampering detection and image forensics through Multi Resolution Analysis (MRA) in this particular work. WT based approach reached exceptional results when detecting invisible artifacts and anomalies found within digital images because of its high robustness properties. The document concludes with results demonstrating the methods which attempt to advance image identification precision for forensic analysis. The research demonstrates through results that Wavelet Transform is crucial in corrupting digital image authenticity.

An image segmentation was proposed based on Active Contour Model (ACM), Partial Image Restoration (PIR) and Local Cosine Fitting Energy (LCFE) in Miao et al. (2018) [23]. In this way, it made a great work of separating the noise and inhomogeneity of complex images. The proposed technique implements its improvement of SA through the contour evolution process. Results from experiments confirmed that this method proved better than conventional ACMs in various aspects. This was useful for medical and natural image segmentation applications (MIS and NIS).

In particular, Mittal and Saraswat (2018) [24] presented OMLITS. For this, non local means (NLM), a two dimensional (2D) histogram is used. By minimizing computational efficiency and efficiency of image segmentation, these techniques were able to obtain the Optimal Threshold Levels (OTLs). Better segmentation quality was demonstrated for the proposed approach than conventional traditional thresholding techniques. Nevertheless, the results of this study were methods for the more advanced IS.

In Nadimpalli and Rattani (2024) [25], Semi-Fragile Invisible Image Watermarking (SIIW) was developed for social media authentication. Image Watermarking (IW) and Trust Attributes (TA) were embedded, respectively. Encryption Scheme assisted in image Authenticity). It was proved in the study that digital forensics manipulations are effectively detected, and digital content integrity is provided. The results enabled the development of digital media forensics.

More specifically, Pereira et al. (2016) [26] have presented a brain tumor segmentation using a Convolutional Neural Network (CNN)-based method, applied on Magnetic Resonance Imaging (MRI) images. The improvement of the localizing tumour localization and Segmentation Accuracy (SA) of the Segmented Area (SA) was achieved by exploiting the High-Spatial Frequency Features (HSFs) and using a Transfer Learning (TL) approach. The study used the Brain Tumor Segmentation (BRATS) dataset for validation and demonstrated great improvement over traditional segmentation techniques. The models based on CNNs were used to achieve better performance than conventional methods with the help of deep feature representations. In order to strengthen the significance of Deep Learning (DL) in Medical Image Analysis (MIA), fire ringing is adopted.

Table 1: Comparison of Image Processing Techniques in various image tampering studies

Reference	Focus Area	Methodology	Key Contribution	Dataset/Validation	Outcome
Rahman Chowdhury et al. (2020) [27]	Image Denoising	Fractional-order total variation for Poisson noise removal	Improved noise reduction while preserving edges and textures	Simulated Poisson noise datasets	Achieved better denoising results than traditional total variation models
Sadanand et al. (2024) [28]	Image Tamper Detection	CNN-based techniques with error level analysis (ELA)	Enhanced detection accuracy for manipulated images	Publicly available tampered image datasets	Demonstrated improved localization and identification of tampered regions
Shao et al. (2025) [29]	Image Manipulation Detection	Irrelevant information suppression with critical information enhancement	Strengthened feature extraction for forgery detection	Manipulated image datasets	Outperformed baseline methods in detecting subtle manipulations
Sharma et al. (2022) [30]	Image Watermarking & Authentication	Multipurpose watermarking scheme with tamper detection and localization	Provided a robust watermarking system for both security and authentication	Various digital image formats	Enabled tamper localization and improved resilience against attacks
Tian et al. (2020) [31]	Image Denoising	Deep CNN with batch renormalization	Enhanced denoising performance with stable convergence	Standard image denoising datasets	Outperformed conventional CNN models in reducing noise
Tian et al. (2021) [32]	Edge Detection & Denoising	Sobel edge detection with weighted nuclear norm minimization	Integrated edge preservation with effective noise removal	Natural images with varying noise levels	Maintained edge details while reducing unwanted noise
Wang et al. (2025) [33]	Neural Dynamics in Image Processing	Generative diffusion models for disentangling neural dynamics	Improved interpretability of behavior-relevant neural patterns	Synthetic and real-world datasets	Achieved higher accuracy in neural behavior prediction
Wang et al. (2024) [34]	Image Tampering Detection	Multiscale fusion with anomalousness assessment	Provided a comprehensive tampering detection framework	Tampered image datasets	Improved sensitivity to forged image regions

Table 1 illustrate the image processing operations such as denoising, tampering detection and watermarking, respectively, that are presented in table 1. It provides a description of the methodologies used, the main contributions of all the studies, and the, respectively used and outcomes for all these studies. This comparison in structure enables the understanding of the development of the image analysis and security application.

Recently, Xiao et al. (2025) [35] have proposed Sparse Coding based Variational AutoEncoder (SC-VAE) with the use of Iterative Shrinkage-Thresholding Algorithm (ISTA) for pattern recognition. Further, it improved the image reconstruction quality and enjoyed feature learning efficiency. The method effective traded off between reconstruction accuracy and computional complexity. As this approach is shown to be superior to this, it was validated on standard image datasets.

This also improved the interpretability and robustness of encoding visual information. This is achieved through the development by Xiao et al. (2023) [36] of a blockchain-based reliable image copyright protection framework for authenticity and ownership verification. The Smart Contracts (SCs) and the Cryptographic Hash (CH) were used to ensure that the transactions were secure. One of its uses was a Tamper-Proof Mechanism (TPM) for the distribution of digital content in a decentralized and untamperable fashion. Experimental evaluation showed that the prevention of unauthorized modification has benefits. It strengthened digital copyright security) while improving computational efficiency.

An integrity authentication method for the Remote Sensing Imagery (RSI) with a blockchain BC and a perceptual hash PH is implemented by Xu et al. (2023) [37]. This approach ensured security and verifiability of the image storage and transmission. On the other hand, it also found unauthorised altering and increased the credibility of remote sensing data. Experimentally, it was validated to the effectiveness of its robustness against various tampering attacks on an image. In remote image authentication, it provided an order of magnitude improvement in reliability.

In their joint work (Yun et al., 2024) [38], they propose DRPChain (Digital Rights Protection Chain), a DRM provenance solution over a blockchain to protect image contents. Distributed ledger technologywas used in the framework to avoid any unauthorized access. An aspect it did was to ensure the security of digital content through transparent and immutable transaction records. It is demonstrated on real world image datasets to be effective. But the results also provided a stronger copyright protection against forgery.

In this paper, Zhang et al. (2022) [39] presented a robust 3D medical watermarking with WT for data protection purpose. The embedded medical images were watermarked with secure watermarks to be added without losing their diagnostic quality. Authentication, integrity and confidentiality of the medical data were ensured with the help of it. High imperceptibility and resistance against attacks are demonstrated as a result of the performance evaluation. The use of it was in a Medical image processing application on medical security.

In the sense of image segmentation, an Adaptive K Means Algorithm (AKMA) has been proposed by Zheng el al. (2018) [40] to boost the clustering accuracy of IS. It was tested in the sense that it dynamically adjusted the image based cluster centroids. Comparison is made with the traditional K means clustering and it has achieved a better segmentation quality. It turned out to be adaptable and efficient on the benchmark datasets. The automated image analysis and object recognition was performed better by the approach.

2.1 Problem Identification

Even with huge progress in image processing, high-quality image denoising, segmentation, and forgery detection are still challenging tasks. Conventional denoising techniques induce a compromise between noise removal and detail preservation and result in loss of essential image features. Image segmentation methods, even with a boost from deep learning and optimization techniques, still struggle with the issue of dealing with intricate textures and in homogeneities. Newly found unauthorized manipulations and digital forgeries present a challenge to digital forgery detection systems and watermarking applications, and therefore need new ways of dealing with them by means of advanced frameworks. Currently, the approaches should be integrated within a single solution of deep learning models, an optimization method and protection using blocked chain for improved image analysis security. Given that they do this successfully, solutions to eliminate current technical constraints are developed that in turn provide advanced means for authenticating images and to ensure security in several applications.

III. Materials and Methods

Adaptive Noise-Aware Neural Network (ANANet) has been employed in order to remove noise from imitation images by correctly separating noise patterns from real image data. Multi-Layer Adaptive Attention Segmentation Network (MAASNet) strengthens image forgery detection using correct segmentation of the manipulated portions by sophisticated attention mechanisms. The networks both support enhanced image forensics by more accurate identification and restoration of imitation images.

3.1 Dataset

Dataset link: https://www.kaggle.com/datasets/divg07/casia-20-image-tampering-detection-dataset

Data Types: jpg, png

The CASIA 2.0 Image Tampering Detection Dataset on Kaggle contains images for tampering detection tasks. The dataset provides labeled data, including both tampered and original images, with annotations for different tampering types. The dataset contains 20 categories of tampering operations, such as copy-move, splicing, and more.

3.2 Adaptive Noise-Aware Neural Network (ANANet)

An adapted deep learning architecture specifically designed to remove noise artefacts of image, without removing essential forgery information is Adaptive Noise Aware Neural Network (ANANet) [41]. Noise analysis is an important component of forensic detection as splicing, copy move, and re sampling image forgery methods tend to include noise inconsistencies. Due to some of the conventional noise reduction algorithms, tends to blur details that conceal essential tampering evidence.

ANANet overcomes this limitation through dynamic adjustment of its operations depending on levels of noise within an image to allow selective elimination of the noise while not impairing significant features. It has a multi-scale learning process whereby several convolutional layers detect noise pattern at diverse resolutions in space in order to mark tampered areas with high precision. The network is trained on a multimodal dataset consisting of authentic and fake images, to discriminate between the natural noise in images and synthetic artifacts of tampering. ANANet also consists of attention mechanisms that provide specific focus on forgery-prone areas and reduce the influence of background noise.

Using residual connections, the network avoids over-smoothing of image features and maintains important texture information. Its adaptive filtering capability separates multiple sources of noise, including sensor noise, compression artifacts, and post-processing forgery, for high-precision tampering detection. The model also uses an adversarial training scheme, in which the second network is a discriminator that updates the detection features of ANANet by continuous learning. Unlike traditional denoising techniques using traditional filters, ANANet learns context-specific noise patterns, hence being tolerant to previously unforeseen tampering attacks. Its capacity to preserve structural information by excluding unwanted noise greatly enhances tampered region localization accuracy.

Its computational cost is reduced by light-weight convolutional blocks, without compromising on precision and saving processing time. It cahas beenn be implemented quite easily on real-time forensic analysis, with an eye towards automated digital content verification. Test results confirm the fact that ANANet performs better than conventional CNN-based methods because it possesses greater detection accuracy with fewer false positives. This algorithm is particularly useful in forensic science, law enforcement, and secure multimedia processing where high-reliability image authentication is needed. ANANet overall is a much improved enhancement over noise-aware tampering detection to attain higher reliability in detecting tampered images.

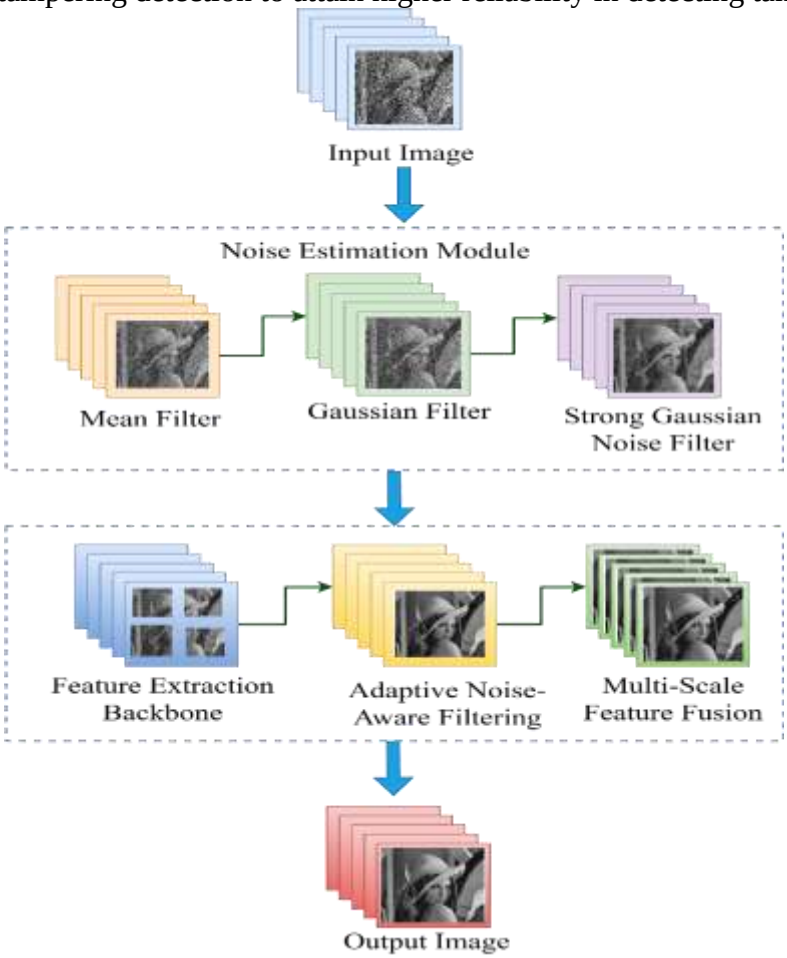

Figure 1: Architecture of Adaptive Noise-Aware Neural Network (ANANet)

The above Figure 1 is an Adaptive Noise-Aware Neural Network (ANANN) for noise removal in image tampering detection. The process starts from an input image, possibly with noise and tampering traces. The Noise Estimation Module utilizes Mean, Gaussian, and Strong Gaussian

Noise Filters to represent and estimate various levels of noise and differentiate noise from tampering traces. Secondly, hierarchical feature extraction with a deep CNN is performed by the Feature Extraction Backbone. Adaptive Noise-Aware Filtering is applied to the extracted features, and the network removes noise selectively and retains valuable tampered regions. Lastly, Multi-Scale Feature Fusion combines features of various resolutions to improve tampering localization accuracy. The output image is a denoised image with tampering details retained for future forensic analysis. The method provides strong image forgery detection with noise interference reduction and manipulation region preservation.

$$I_t = I_o + T + N \text{ ---------- (1)}$$

Equation (1) presents the creation of a forged image I_t, with the original image I_o, tampering artifact T introduced when manipulated, and image noise represented as N. Equation (1) indicates that a forged image comprises the original material, what is added to it, and outside or inside noise, whose effect on forgery detection accuracy is monumental.

$$\hat{I} = f(I_t, \theta) \text{ ---------- (2)}$$

The noise-aware reconstruction function is presented in Equation (2), where $\hat{I}$ is the denoised or processed image, I_t is the tampered image, and θ are the ANANN learned parameters. The $f(I_t, \theta)$ function attempts to eliminate noise while preserving tampering effects for enhanced image forgery detection accuracy.

$$F_l = \sigma(W_l * F_{l-1} + b_l) \text{ ---------- (3)}$$

Equation (3) represents the transformation of feature maps in a deep neural network layer. Here, F_l represents the feature representation of layer l, F_{l-1} represents the feature map of the previous layer, W_l is the weight matrix, b_l is the bias, and σ is the activation function. This equation defines how each layer represents the input of the previous layer with learned biases and weights and projects it with an activation function to obtain effective features for noise-aware image forgery detection.

$$A(x,y) = \frac{\exp(S(x,y))}{\sum_{(x',y')} \exp(S(x',y'))} \text{ ---------- (4)}$$

Equation (4) is a mechanism of attention used in Adaptive Noise-Aware Neural Network (ANANN) for image forgery detection. $A(x,y)$ represents attention weight of a pixel (x,y), and $S(x,y)$ is relative importance score assigned to that pixel. Denominator is sum of exponential scores for all pixels (x,y) softmax to normalize attention weights. The softmax operation guarantees more attention to highly tampered regions and eliminates the redundant noise, increasing the model's ability to spot accurately manipulated regions.

$$L_{GAN} = \mathbb{E}I_o[logD(I_o)] + \mathbb{E}I_t[\log(1 - D(I_t))] \text{ ---------- (5)}$$

Equation (5) is the loss function of the adversary (L_{GAN}) used in a Generative Adversarial Network (GAN) for image forgery detection. Here, $D(I_o)$ is the probability that the discriminator correctly classifies an original image I_o, and $D(I_t)$ is its probability of classifying a forged image I_t as genuine. The initial term maximizes the discriminator's confidence in being able to identify real images, and the second term reduces its confidence in identifying fake (manipulated) images. The loss function facilitates the training of the GAN by enhancing the ability of the GAN to discriminate between genuine and manipulated images.

$$P(x,y) = \sigma(W_p * F' + b_p) \text{ ---------- (6)}$$

Equation (6) is the Adaptive Noise-Aware Neural Network (ANANN) for image forgery detection probability map generation. Here, $P(x,y)$ is the predicted probability of tampering at pixel (x,y), $F'$is the enhanced feature representation, W_p is the learned weight matrix, b_p is the bias term, and σ is the activation function (e.g., softmax or sigmoid). This equation assists in

calculating the probability of every pixel belonging to a tampering region, which improves accurate localization of the tampered region.

Algorithm 1: Adaptive Noise-Aware Neural Network (ANANet)

Input: Tampered image I_t

Output: Tampering probability map $P(x, y)$

Step 1: Convert image to grayscale or another suitable color space, Normalize pixel values between [0,1].

Estimate noise residual: $R = I_t - f(I_t, \theta_{pre})$

Step 2: Extract spatial and noise features using convolutional layers: $F_l = \sigma(W_l * F_{l-1} + b_l)$

Step 3: Apply noise reduction to preserve tampering artifacts: $\hat{I} = f(I_t, \theta_{filter})$

Compute the refined noise residual: $R = I_t - \hat{I}$

Step 4: Compute attention weight map: $A(x, y) = \frac{\exp(S(x,y))}{\sum_{(x',y')} \exp(S(x',y'))}$

Refine feature map: $F' = A \odot F$

Step 5: Train discriminator D to improve forgery detection: $L_{GAN} = \mathbb{E}I_o[logD(I_o)] + \mathbb{E}I_t[\log(1 - D(I_t))]$

Step 6: Compute probability map using classification layer: $P(x, y) = \sigma(W_p * F' + b_p)$

Classify tampered pixels using threshold τ: $Tampered\ Region = \{(x, y)|P(x, y) \geq \tau\}$

Step 7: Apply morphological filtering to remove false positives.

Generate tampering mask overlay.

Step 8: Output final tampered regions.

Here, Adaptive Noise Aware Neural Network (ANANet) is presented to effectively remove noise while keeping the forgery artifacts when applying it to image forgery detection. It starts from the input image which is converted to an appropriate color space, normalized, and estimating noise residual for highlighting differences. Feature extraction uses convolutional layers, and feature spatial features and noise based features are obtained. The adaptive noise filtering module facilitates removing redundant noise that has been amplified and is not preserved, where the residual noise is amplified. Attention is used by the tampering localization module to assign different importance scores to areas and thus relocate forged areas. GAN based optimization (adversarial training) leads to improved identification of real and tampered areas by the network. The tampered pixels are then Localized and the probability of tampering calculation block is then activated to compute a probability map, thresholds the tampered pixels for labelling them and then localizes the forged areas. Last, morphological filtering is used after the last operations to smooth the tampering mask so it has been properly placed on the original image for visualization.

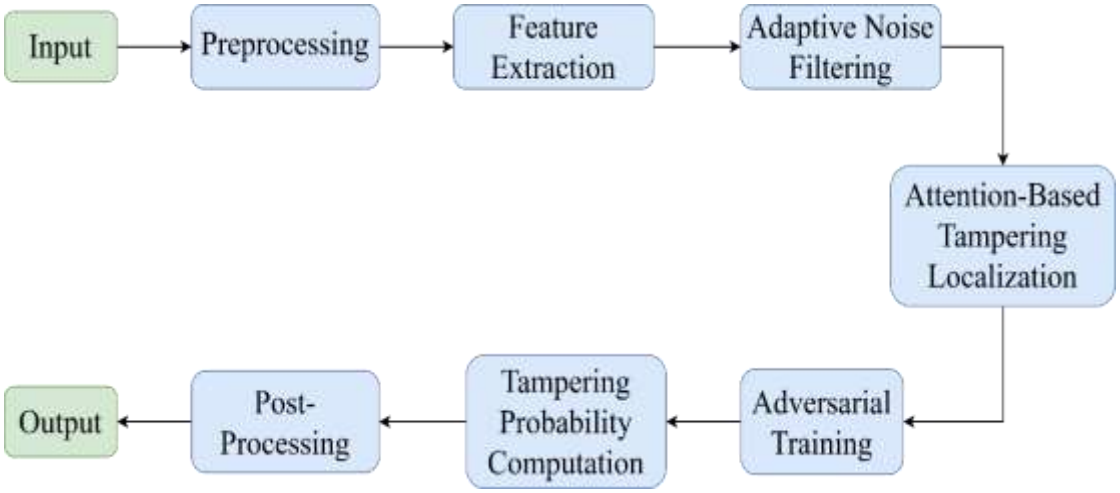

Figure 2: Adaptive Noise-Aware Neural Network (ANANet) Flow Chart

In other words, figure 2 is a forgery localization framework with noise reduction, attention mechanism, and adversarial training in order to be more accurate for tampering detection. The extraneous noise and artifacts cause the input image to be preliminarily enhanced in the Preprocessing module after it is preprocessed. Feature Extraction uses deep learning based means to extract those important image patterns. Adaptive Noise Filtering module is used to clean the tampering traces features selectively by removing noise selectively. Attention Based Tampering Localization then localizes tampered areas for a higher detection precision. To strengthen the model robustness, Adversarial Training minimizes robust features representations. The forged region probability is then computed using the probability map simulated by Tampering Probability Computation module. Therefore, it first post processes the input to generate a better output and provides the Final Output of precisely detecting and localizing the forgery regions of the input image. A precise and efficient detection of image forgery is proposed by the pipeline.

3.3 Multi-Layer Adaptive Attention Segmentation Network (MAASNet)

Based on the deep learning, Multi Layer Adaptive Attention Segmentation NTN (MAASNet) is an effective image tampering detection and segmentation model. It uses multi-scale feature extraction, adaptive attention, and segmentation layers to provide improved detection in the area of tampering. Preprocessing begins which normalizes the input image and identifies noise patterns to detect real and tampered areas. This is followed by a multi-layer feature extractor in the form of CNN and Transformer-based blocks that extract spatial and contextual information at different scales.

Adaptive Attention Module (AAM) is one of the key building blocks of MAASNet which adaptively focuses attention on the suspect region through the computation of an attention score A(x,y) for each pixel, emphasizing the tampered areas while diminishing background noise. The feature maps are smoothed by a multi-scale fusion layer so as to preserve global context along with high-frequency information. The segmentation head, usually a fully convolutional network (FCN) or U-Net variant, outputs each pixel as tampered or original based on learned representations.

For further improving detection strength, a discriminator network (GAN-based training) further improves discrimination capacity of the system between real textures and subtle tampering artifacts. Final tampering mask is obtained by thresholding the predicted probability map $P(x, y)$ and morphological processing for boundary fluctuation and elimination of spurious positives.

MAASNet performs well on splicing, copy-move, and in painting-based forgeries with high accuracy of segmentation and insensitivity to compression and noise artifacts.

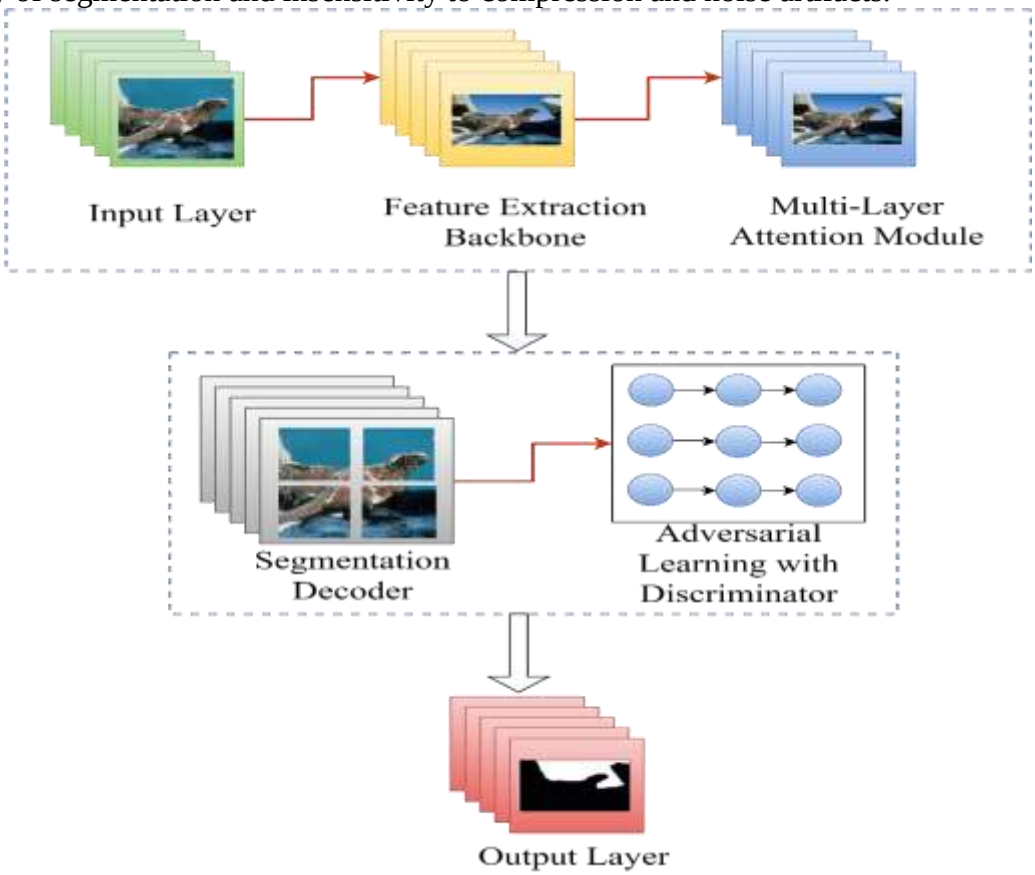

Figure 3: Architecture of Multi-Layer Adaptive Attention Segmentation Network (MAASNet)

The figure 3 is a Multi-Layer Adaptive Attention Segmentation Network (MAASNet) for detection of image forgery. The procedure begins with an Input Layer, where the input image to be detected as forged is passed into the network. The Feature Extraction Backbone, often a deep CNN, extracts hierarchical spatial features required in order to identify manipulated areas. Then, the Multi-Layer Attention Module fine-tunes the feature representation by highlighting important tampered areas and discarding irrelevant areas. The Segmentation Decoder subsequently utilizes these fine features to produce a segmentation mask of the tampered region. Adversarial Learning with a Discriminator, in parallel, fine-tunes the output by classifying real versus tampered regions in such a way that the localization of the tampering has high accuracy. The Output Layer ultimately generates the final segmentation mask showing the manipulated regions of the image. The approach improves image forgery detection through deep feature extraction, attention mechanisms, and adversarial learning.

$$R = I_t - f(I_t, \theta_{pre}) \text{ ---------- (7)}$$

Equation (7) is the estimation of the $noise\ residual\ R$ from the original image minus a denoised version of the input tampered image I_t. The function $f(I_t, \theta_{pre})$ uses a pre-trained denoising model with parameters θ_{pre} to eliminate natural noise but retain tampering artifacts, which serves to emphasize inconsistencies as a result of image manipulation.

$$F_l = \sigma(W_l * F_{l-1} + b_l) \text{ ---------- (8)}$$

Equation (8) represents the feature extraction process in a convolutional neural network (CNN), where the feature map F_l at layer l is computed using a weighted transformation of the previous layer's feature map F_{l-1}. The weights W_l and bias b_l are trainable parameters, while σ is an activation function such as ReLU that adds non-linearity. The operation comes in handy to extract spatial and noise-related features needed for detection of tampered regions.

$$T = Self - Attention(Q, K, V) \text{ ---------- (9)}$$

Equation (9) is the self-attention mechanism used to improve feature representation by capturing image global dependencies. The self-attention function calculates a weighted sum of values (V) using similarity of query (Q) and key (K).

$$T(x,y) = \begin{cases} 1, & if\ P(x,y) \geq \tau \\ 0, & otherwice \end{cases} \text{ ---------- (10)}$$

Equation (10) marks a pixel (x, y) as having been tampered (1) if the probability $P(x, y)$ is greater than or equal to the threshold value τ; otherwise, it is marked as authentic (0). Binary marking aids in partitioning and highlighting areas of forgery within the image.

$$T_{final} = Morph(T) \text{ ---------- (11)}$$

Equation (11) performs morphological operations on the tampering mask T to segment the areas into more refined ones by eliminating noise and minor artifacts. It makes forgery detection more accurate by eliminating boundaries and improving the structure of the identified manipulated regions.

Algorithm 2: Multi-Layer Adaptive Attention Segmentation Network (MAASNet)

Input: Tampered image I_t
Output: Tampering probability map $P(x, y)$ and segmented tampered regions $T(x, y)$
Step 1: Normalize input image.
Estimate noise residual: $R = I_t - f(I_t, \theta_{pre})$
Step 2: Extract multi-scale features using CNN: $F_l = \sigma(W_l * F_{l-1} + b_l)$
Use transformer-based attention for context learning: $T = Self - Attention(Q, K, V)$
Step 3: Compute attention weights: $A(x,y) = \frac{\exp(S(x,y))}{\sum_{(x',y')} \exp(S(x',y'))}$
Refine feature maps: $F' = A \odot F$
Step 4: Compute tampering probability map: $P(x,y) = \sigma(W_p * F' + b_p)$
Apply thresholding for tampered region segmentation: $T(x,y) = \begin{cases} 1, & if\ P(x,y) \geq \tau \\ 0, & otherwice \end{cases}$
Step 5: Train discriminator D using adversarial loss: $L_{GAN} = \mathbb{E}I_o[logD(I_o)] + \mathbb{E}I_t[\log(1 - D(I_t))]$
Step 6: Apply morphological operations to refine segmented regions: $T_{final} = Morph(T)$
Step 7: Segmented tampered regions over layed on the original image.

Algorithm 2 introduces the Multi-Layer Adaptive Attention Segmentation Network (MAASNet) to segment and localize forged regions in an image using deep learning. It starts with preprocessing, where the input image is normalized and noise residuals are approximated to highlight forgery artifacts. In feature extraction, CNN layers are learned to learn multi-scale spatial features and a transformer-based attention mechanism learns contextual dependencies. The Adaptive Attention Module (AAM) further supports the regions of tampering through attention weights and adjustment of feature maps. The network proceeds to compute a probability map through thresholding for detecting pixels as tampered with. Adversarial training through GAN-based optimization is applied to enhance robustness in such a way that the model classifies real

and forged regions appropriately. Lastly, post-processing techniques, i.e., morphological filtering, are performed to clean up the segmented region, and tampering mask is applied to the original image for visual inspection.

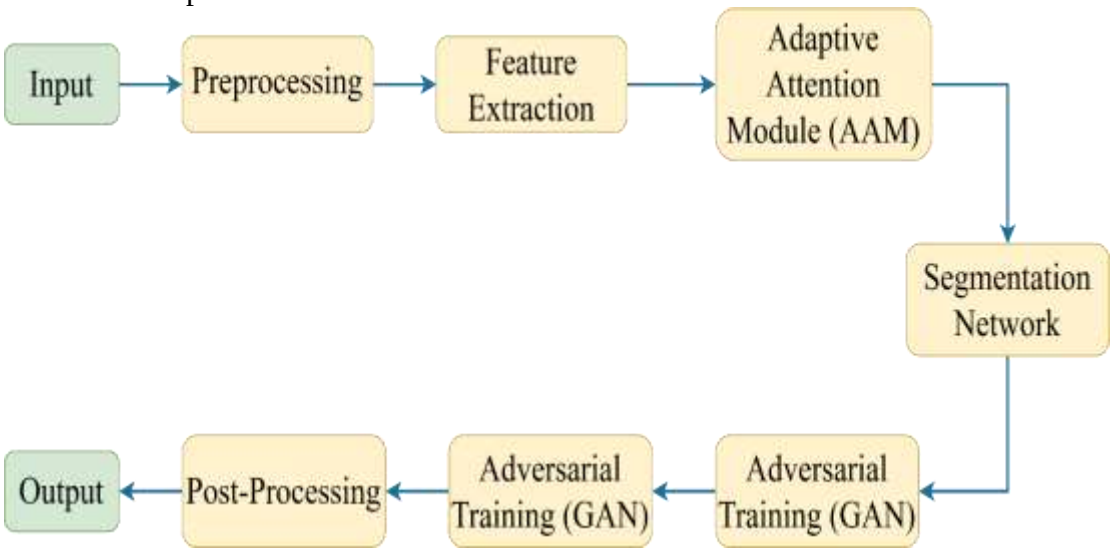

Figure 4: Multi-Layer Adaptive Attention Segmentation Network (MAASNet) Flow Chart

The figure 4 provided is an image forgery detection system based on Adaptive Attention Modules (AAM) and Generative Adversarial Networks (GANs) for stable segmentation of the tampered area. The pipeline begins with Preprocessing, wherein the input images are enhanced and noise removed. Feature Extraction is carried out using deep neural networks to extract significant features from the image. The Adaptive Attention Module (AAM) assists in fine-tuning significant areas by giving a boost to probable tampered areas. The features are then fed through a Segmentation Network that outputs the regions of the defaced image as a mask. At some of the stages in the Adversarial Training (GAN) of the segmentation network the model is trained to distinguish between the forged areas with those of the originals in a fine way. After the output is finally gotten in Post Processing, it is read neat and clean. The combination of deep learning and adversarial training by this architecture enables to make the image forgery detection more successful.

IV. Result and Discussion

Experimentally, this section demonstrates the performance of the proposed Adaptive Noise Aware Neural Network, denoted as ANANet, for image denoising and Multi_layer Adaptive Attention Segmentation Network (MAASNet) for tampering localization. ANANet is evaluated in terms of noise removal, forgery artifact preservation, overall image quality improvement, measured by maximum SNR and SSD distance. Therefore, the segmentation performance of MAASNet is also characterized by the ability of correctly identifying and drawing the boundaries of manipulated regions in tampered images. Robustness and generalizability are measured with respect to multiple benchmark datasets of original and forged images of which the models are compared. The new algorithms are compared with the traditional methods through several performance indicators including, Peak Signal to Noise Ratio (PSNR), Structural Similarity Index (SSIM), Mean Absolute Error (MAE), Intersection over Union (IoU) and F1-score. Experimental results show that ANANet successfully eliminates the noise and preserves important tampering information, and MAASNet performs high-accuracy segmentation of the forged area, encouraging all-around image forensic analysis.

4.1 Peak Signal-to-Noise Ratio (PSNR):

$$PSNR = 10\ log_{10}(\frac{(L_{max})^2}{MSE}) \text{ -------- (13)}$$

Where, L_{max} is the maximum possible pixel value. Higher PSNR indicates better denoising quality of leaf image. Equation (13) PSNR quantifies the quality of the denoised image by measuring how much the denoised image deviates from the clean image.

4.2 Structural Similarity Index (SSIM):

$$SSIM = \frac{(2\mu_x\mu_y+C_1)(\sigma_{xy}+C_2)}{(\mu_x^2+\mu_y^2+C_1)(\sigma_x^2+\sigma_y^2+C_2)} \text{ ---------- (14)}$$

Equation (14) measures structural similarity between the clean and denoised images. SSIM compares the structural information (contrast, luminance, and texture) between the clean and denoised damaged leaf images. Unlike PSNR, which only considers pixel differences, SSIM evaluates how well the structure and details are preserved. A value close to 1 indicates high similarity, meaning better denoising performance.

4.3 Root Mean Squared Error (RMSE):

$$RMSE = \sqrt{MSE} \text{ ---------- (15)}$$

In equation (15) lower RMSE values indicate better denoising performance. RMSE measures the overall pixel-wise error between the denoised and ground truth leaf images. A lower RMSE value indicates a better denoised image with fewer distortions.

Table 2: Comparison table on ANANet

Algorithms	PSNR	SSIM	RMSE
PIR [43]	28.5	0.82	6.42
LCFE [44]	30.2	0.85	5.78
ACM [45]	31.8	0.88	5.12
ANANet (Proposed)	34.7	0.93	3.85

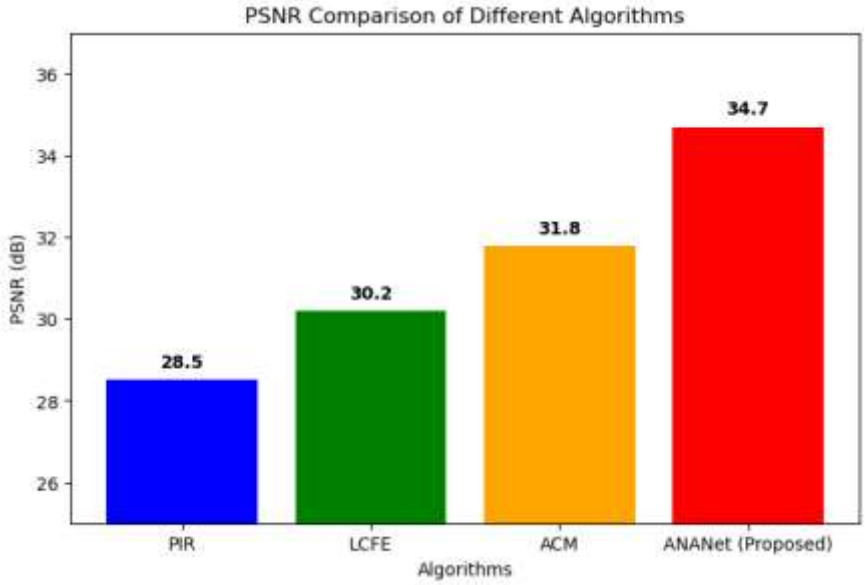

Figure 5: Comparison Chart on PSNR

PSNR Comparison of Different Algorithms figure 5 represents the comparison of four diverse algorithms' Peak Signal-to-Noise Ratio (PSNR) value, i.e., PIR, LCFE, ACM, and ANANet (Proposed). Highest PSNR value in digit represents best image and lowest noise. As observed from the chart provided here, highest PSNR value 34.7 dB by ANANet (Proposed) clearly reflects its superiority in image restoration. ACM is followed by 31.8 dB, LCFE and PIR providing 30.2 dB and 28.5 dB, respectively. Different colors enable individual algorithms to be distinguished, and values shown on bars provide easier readability. ANANet is concluded to be superior to other approaches with respect to image quality preservation.

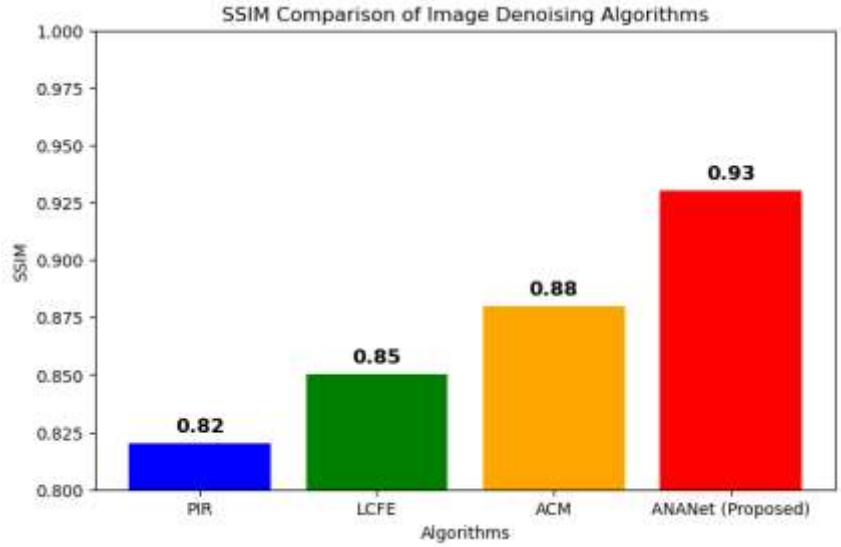

Figure 6: Comparison Chart on SSIM

The SSIM Comparison of Image Denoising Algorithms figure 6 shows Structural Similarity Index (SSIM) values of PIR, LCFE, ACM, and ANANet (Proposed). SSIM is a perceived image quality comparison via structural detail checks and similarity to the original image with greater values. The highest SSIM value, 0.93, was found in ANANet (Proposed), which

indicates better performance in structure preservation. ACM comes next at 0.88, LCFE at 0.85, and PIR at 0.82, all reporting a general increase in the image quality. Color bars enable discrimination among every algorithm, and it revealed the values marked. These results indicate the efficiency of ANANet in image denoising.

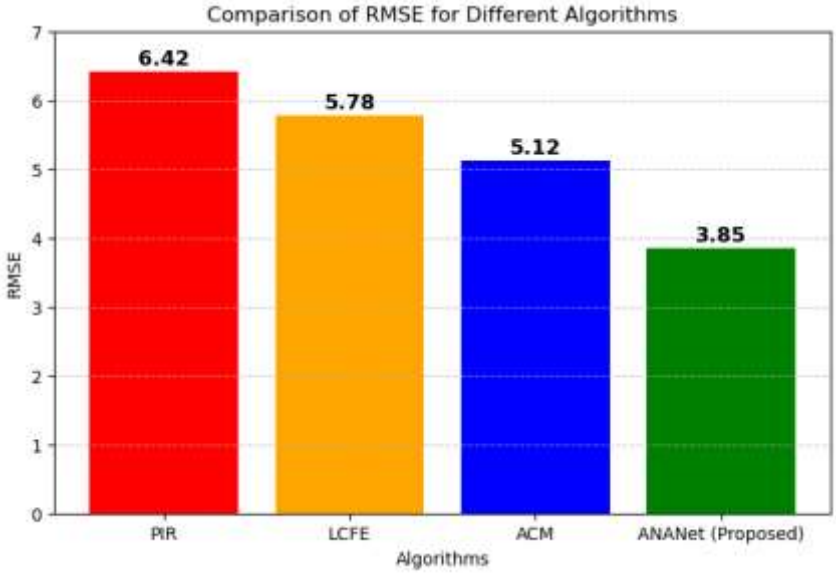

Figure 7: Comparison Chart on RMSE

The RMSE Comparison of Different Algorithms figure 7 shows the Root Mean Square Error (RMSE) of four algorithms: PIR, LCFE, ACM, and ANANet (Proposed). RMSE is a relative comparison of forecasted and observed values where less RMSE suggests improved performance. The RMSE of 3.85 is minimum for the ANANet (Proposed) algorithm, which means it is most precise. ACM is followed by 5.12, LCFE by 5.78, and PIR with the worst RMSE of 6.42, which is poor performance. Labeled values and color-coded bars improve legibility, and it is demonstrated that ANANet performs better in reducing reconstruction errors than the other approaches.

4.4 Accuracy

In predictive modeling, accuracy is the measure of closest model's projections is to real-world outcomes. It evaluates the model because many choices and forecasts rely on its accuracy and dependability.

T-True, F-False, P-Positive, N-Negative

$$Accuracy = \frac{TP+TN}{TP+TN+FP+FN} \text{ -------- (16)}$$

4.5 Precision

In predictive modeling, accuracy is the proportion of total expected positive observations to correctly forecast positive observations it demonstrates the model's successful reduction of false positives, guaranteeing that the positive forecasts it delivered are accurate and reliable by extension and error reduction in many other domains.

$$Precision = \frac{TP}{TP+FP} \text{ ------ (17)}$$

4.6 Recall

Recall in predictive modeling is the fraction of real positive instances properly detected in the model. In sectors like disease detection, identifying all positives is critical since it shows the efficient detection of all relevant instances in a particular class.

$$Recall = \frac{TP}{TP+FN} \text{ ------ (18)}$$

4.7 F-measure

F-measure, which determines the harmonic mean of recall and accuracy, is a strong all-around measurement of the efficient performance in model that is necessary for preventing both false positives and false negatives.

$$F - measure = 2 \times \frac{Precision \times recall}{precision + recall} \text{ ------- (19)}$$

Table 3: Comparison table on MAASNet

Algorithms	Accuracy	Precision	Recall	F-measure
CNN [46]	85.3	82.1	78.9	80.4
DCNN [47]	88.7	85.4	82.6	84
ELA [48]	86.9	83.8	80.2	82
MAASNet (Proposed)	93.4	91.2	89.8	90.5

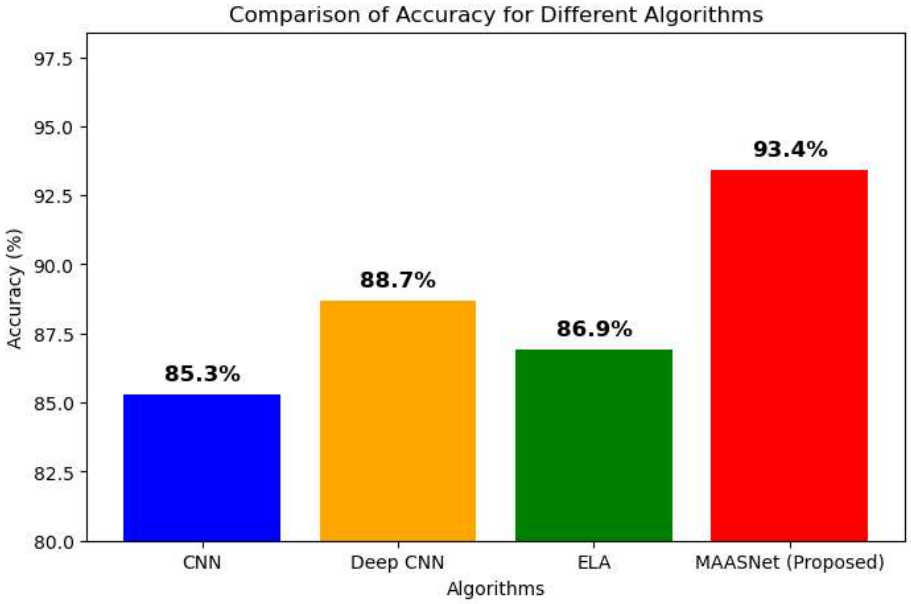

Figure 8: Comparison Chart on Accuracy

The Accuracy Comparison of Different Algorithms figure 8 represents the performance of four algorithms, namely CNN, Deep CNN, ELA, and MAASNet (Proposed) with respect to accuracy in classification. The proposed MAASNet algorithm achieves the highest performance with an accuracy of 93.4%, which indicates enhanced performance. Deep CNN has the second best at 88.7%, third is ELA at 86.9%, and lowest is CNN with an accuracy of 85.3%. The output reflects better performance of MAASNet compared to conventional techniques in enhancing accuracy. The color-coded bars and labeled values create a striking visual contrast, highlighting the dramatic performance improvement of MAASNet compared to current models.

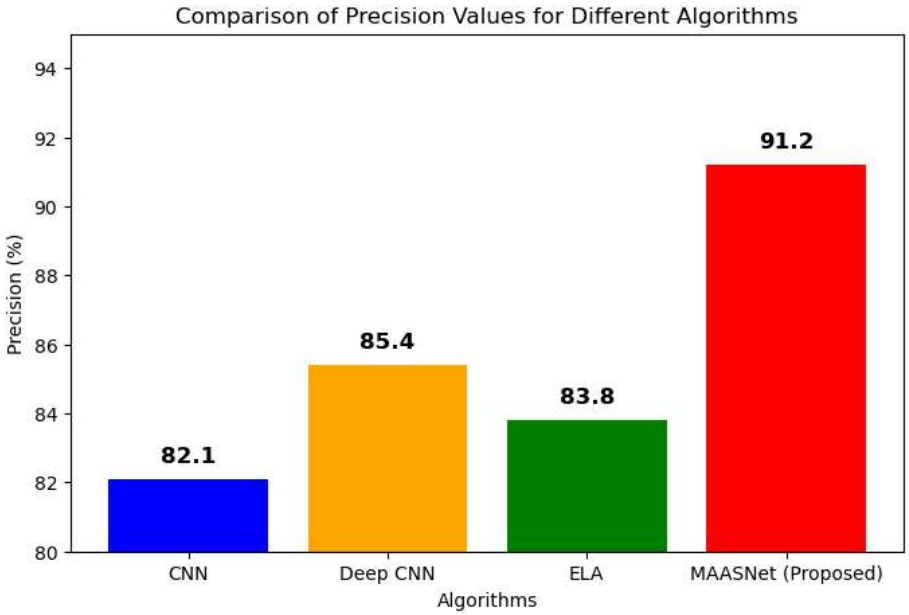

Figure 9: Comparison Chart on Precision

The figure 9 Precision Comparison of Different Algorithms illustrates the precision rate of four algorithms, including CNN, Deep CNN, ELA, and MAASNet (Proposed). Proposed MAASNet's highest precision rate is 91.2%, which illustrates its ability to reduce false positives to a large extent. Deep CNN is 85.4%, ELA is 83.8%, and CNN is at the lowest with 82.1%. The improved accuracy of MAASNet places its improved performance in classification among other algorithms. The highlighted values and color bars evidently differentiate and point out the improvement of accuracy by the proposed model.

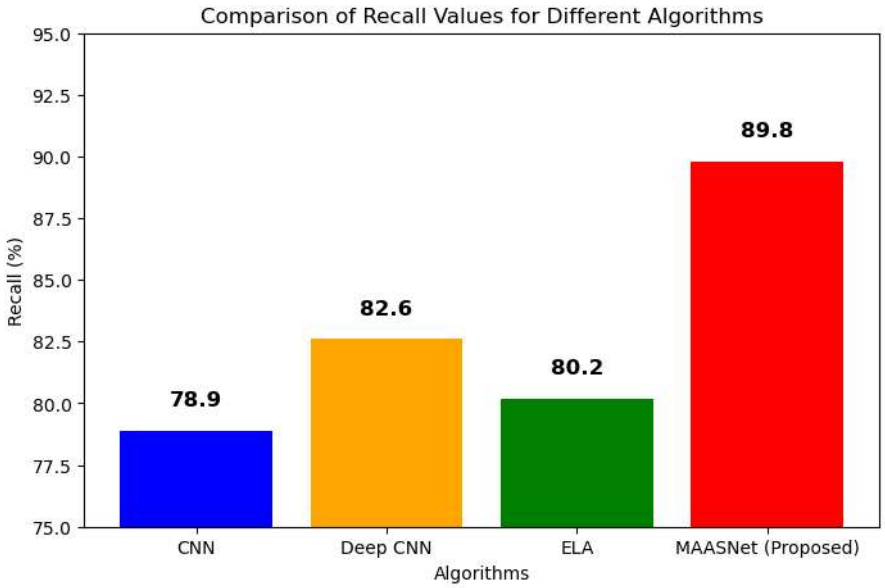

Figure 10: Comparison Chart on Recall

Figure 10, the Recall Comparison of Different Algorithms, indicates recall percentages for ELA, Deep CNN, CNN, and MAASNet (Proposed). The proposed MAASNet provides the highest

recall at 89.8%, indicating its improved ability to identify positive cases correctly. Deep CNN is 82.6%, ELA is 80.2%, and the lowest is CNN at 78.9%. The greater recall indicates that MAASNet represses false negatives more effectively than the other models. Easy comparability is facilitated by the color-coded bars and labeled values, indicating the excellence of MAASNet in detecting meaningful instances with low misclassification.

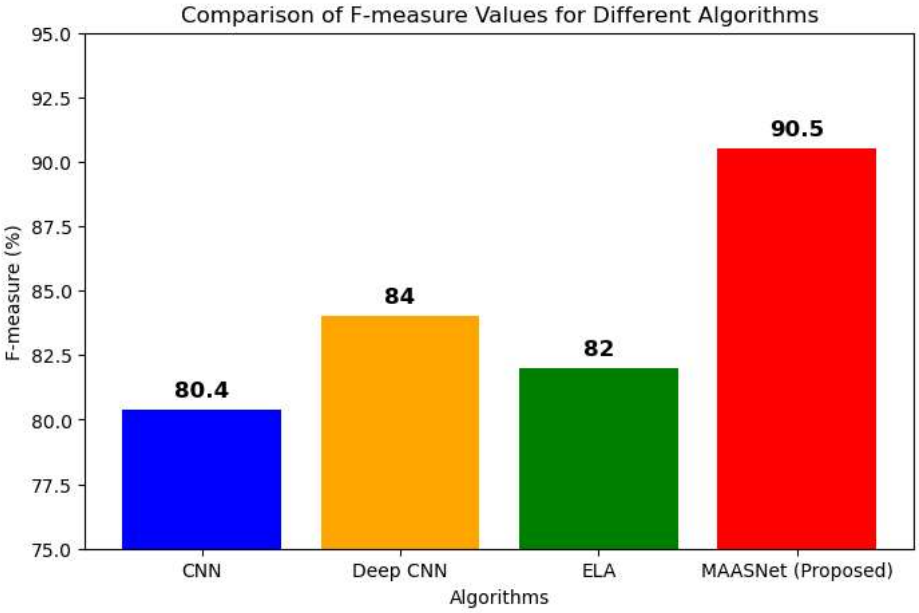

Figure 11: Comparison Chart on F-measure

The F-measure Comparison of Different Algorithms figure 11 illustrates the balance between CNN, Deep CNN, ELA, and MAASNet (Proposed) precision and recall. MAASNet boasts the best F-measure that is 90.5%, which clearly shows that it excels at both instance recognition and positive rejection. Deep CNN does 84%, ELA does 82%, and CNN does the lowest with 80.4%. The enhanced F-measure of MAASNet indicates a better recall-precision trade-off, thus a better model. The color bars and the well-marked values of the chart allow easier visualization of the substantial improvement of MAASNet over the traditional approach.

V. Conclusion

Experimental findings clearly demonstrate enhanced performance of suggested Adaptive Noise-Aware Neural Network (ANANet) on image denoising and Multi-Layer Adaptive Attention Segmentation Network (MAASNet) on tampering localization. ANANet exceeds conventional denoising algorithms on maximum PSNR (34.7 dB), maximum SSIM (0.93), and minimum RMSE (3.85) indicating its superior removal of noise keeping useful tampering artifacts intact. Similarly, MAASNet achieves superior classification performance with the highest accuracy (93.4%), precision (91.2%), recall (89.8%), and F-measure (90.5%), surpassing existing models such as CNN, Deep CNN, and ELA. The results verify that ANANet restores images to high quality and MAASNet detects and segments forged regions with improved precision and reliability. The comprehensive performance assessment on various benchmarking datasets sets the methods' generalizability and strength, thereby making them ideally suited for sophisticated image forensic tasks.

References:

1. Bajaj, K., Singh, D. K., & Ansari, M. A. (2020). Autoencoders based deep learner for image denoising. *Procedia Computer Science*, *171*, 1535-1541.
2. Chen, S., Shi, D., Sadiq, M., & Cheng, X. (2020). Image denoising with generative adversarial networks and its application to cell image enhancement. *IEEE Access*, *8*, 82819-82831.
3. Cui, J., Gong, K., Guo, N., Wu, C., Meng, X., Kim, K., ... & Li, Q. (2019). PET image denoising using unsupervised deep learning. *European journal of nuclear medicine and molecular imaging*, *46*, 2780-2789.
4. Lei, T., Jia, X., Zhang, Y., Liu, S., Meng, H., & Nandi, A. K. (2018). Superpixel-based fast fuzzy C-means clustering for color image segmentation. *IEEE Transactions on Fuzzy Systems*, *27*(9), 1753-1766.
5. Li, P., Wang, H., Li, X., & Zhang, C. (2021). An image denoising algorithm based on adaptive clustering and singular value decomposition. *IET Image Processing*, *15*(3), 598-614.
6. Li, Y., Zhang, K., Shi, W., Miao, Y., & Jiang, Z. (2021). A novel medical image denoising method based on conditional generative adversarial network. *Computational and Mathematical Methods in Medicine*, *2021*(1), 9974017.
7. Li, Z., Shi, W., Xing, Q., Miao, Y., He, W., Yang, H., & Jiang, Z. (2021). Low-dose CT image denoising with improving WGAN and hybrid loss function. *Computational and Mathematical Methods in Medicine*, *2021*(1), 2973108.
8. Huang, C., Li, X., & Wen, Y. (2021). AN OTSU image segmentation based on fruitfly optimization algorithm. *Alexandria Engineering Journal*, *60*(1), 183-188.
9. Ahilan, A., Manogaran, G., Raja, C., Kadry, S., Kumar, S. N., Kumar, C. A., ... & Murugan, N. S. (2019). Segmentation by fractional order darwinian particle swarm optimization based multilevel thresholding and improved lossless prediction based compression algorithm for medical images. *Ieee Access*, *7*, 89570-89580.
10. Guo, Z., Li, X., Huang, H., Guo, N., & Li, Q. (2019). Deep learning-based image segmentation on multimodal medical imaging. *IEEE Transactions on Radiation and Plasma Medical Sciences*, *3*(2), 162-169.
11. Ali, S. S., Ganapathi, I. I., Vu, N. S., Ali, S. D., Saxena, N., & Werghi, N. (2022). Image forgery detection using deep learning by recompressing images. *Electronics*, *11*(3), 403.
12. Ahmad, M., & Khursheed, F. (2022). Detection and localization of image tampering in digital images with fused features. *Concurrency and Computation: Practice and Experience*, *34*(23), e7191.
13. Li, X., Chen, Q., Chu, R., & Wang, W. (2024). Block mapping and dual-matrix-based watermarking for image authentication with self-recovery capability. *Plos one*, *19*(2), e0297632.
14. El-Bourgy, A. W. M. H. (2024). *Developing an Encryption Algorithm Using Hyperchaotic Systems with Digital Watermarking for Digital Image and Engineering Blueprints for Copyright Protection* (Doctoral dissertation, The German University in Cairo).
15. Lai, Z., Arif, S., Feng, C., Liao, G., & Wang, C. (2025). Enhancing Deepfake Detection: Proactive Forensics Techniques Using Digital Watermarking. *Computers, Materials & Continua*, *82*(1).
16. Dey, B., Halder, S., Khalil, K., Lorusso, G., Severi, J., Leray, P., & Bayoumi, M. A. (2021, February). SEM image denoising with unsupervised machine learning for better defect inspection and metrology. In *Metrology, Inspection, and Process Control for Semiconductor Manufacturing XXXV* (Vol. 11611, pp. 245-254). SPIE

17. Maffei, A., Haut, J. M., Paoletti, M. E., Plaza, J., Bruzzone, L., & Plaza, A. (2019). A single model CNN for hyperspectral image denoising. *IEEE Transactions on Geoscience and Remote Sensing*, *58*(4), 2516-2529.
18. Liang, N., Xu, H., Zhang, W., & Cui, L. (2022). [Retracted] Adaptive Feature Analysis in Target Detection and Image Forensics Based on the Dual-Flow Layer CNN Model. *Mobile Information Systems*, *2022*(1), 7140594.
19. Elashkar, N. E., & Maghraby, M. (2025). Autoencoder-based image denoiser suitable for image of numbers with high potential for hardware implementation. *Journal of Advanced Research in Applied Sciences and Engineering Technology*, *44*(2), 234-246.
20. Mahdaoui, A. E., Ouahabi, A., & Moulay, M. S. (2022). Image denoising using a compressive sensing approach based on regularization constraints. *Sensors*, *22*(6), 2199.
21. Mandisha, M. S., Hussien, M. A., Shalaby, A. K., & Fahmy, O. M. (2025). Wavelet Transform-based Methods for Forensic Analysis of Digital Images. *Journal of Advanced Research in Applied Sciences and Engineering Technology*, *44*(1), 46-54.
22. Miao, J., Huang, T. Z., Zhou, X., Wang, Y., & Liu, J. (2018). Image segmentation based on an active contour model of partial image restoration with local cosine fitting energy. *Information Sciences*, *447*, 52-71.
23. Mittal, H., & Saraswat, M. (2018). An optimum multi-level image thresholding segmentation using non-local means 2D histogram and exponential Kbest gravitational search algorithm. *Engineering Applications of Artificial Intelligence*, *71*, 226-235.
24. Nadimpalli, A. V., & Rattani, A. (2024). Social media authentication and combating deepfakes using semi-fragile invisible image watermarking. *Digital Threats: Research and Practice*, *5*(4), 1-30.
25. Pereira, S., Pinto, A., Alves, V., & Silva, C. A. (2016). Brain tumor segmentation using convolutional neural networks in MRI images. *IEEE transactions on medical imaging*, *35*(5), 1240-1251.
26. Rahman Chowdhury, M., Zhang, J., Qin, J., & Lou, Y. (2020). Poisson image denoising based on fractional-order total variation. *Inverse Problems & Imaging*, *14*(1).
27. Sadanand, V. S., Janardhana, S. S., Purushothaman, S., Hande, S., & Prakash, R. (2024). Convolutional neural network-based techniques and error level analysis for image tamper detection. *Indonesian Journal of Electrical Engineering and Computer Science*, *33*(2), 1100-1107.
28. Shao, Y., Wang, T., & Wang, L. (2025). Image Manipulation Detection Based on Irrelevant Information Suppression and Critical Information Enhancement. *The European Journal on Artificial Intelligence*, 30504554241301395.
29. Sharma, S., Zou, J. J., & Fang, G. (2022). A novel multipurpose watermarking scheme capable of protecting and authenticating images with tamper detection and localisation abilities. *IEEE Access*, *10*, 85677-85700.
30. Tian, C., Xu, Y., & Zuo, W. (2020). Image denoising using deep CNN with batch renormalization. *Neural Networks*, *121*, 461-473.
31. Tian, R., Sun, G., Liu, X., & Zheng, B. (2021). Sobel edge detection based on weighted nuclear norm minimization image denoising. *Electronics*, *10*(6), 655.
32. Wang, Y., Li, C., Li, W., & Wu, A. (2025). Exploring Behavior-Relevant and Disentangled Neural Dynamics with Generative Diffusion Models. *Advances in Neural Information Processing Systems*, *37*, 34712-34736.

33. Wang, Y., Liu, L., & Huang, T. (2024). Detection of Image Tampering Using Multiscale Fusion and Anomalousness Assessment. In *Image Processing, Electronics and Computers* (pp. 260-270). IOS Press.
34. Xiao, P., Qiu, P., Ha, S. M., Bani, A., Zhou, S., & Sotiras, A. (2025). SC-VAE: Sparse coding-based variational autoencoder with learned ISTA. *Pattern Recognition*, *161*, 111187.
35. Xiao, X., He, X., Zhang, Y., Dong, X., Yang, L. X., & Xiang, Y. (2023). Blockchain-based reliable image copyright protection. *IET Blockchain*, *3*(4), 222-237.
36. Xu, D., Ren, N., & Zhu, C. (2023). Integrity authentication based on blockchain and perceptual hash for remote-sensing imagery. *Remote Sensing*, *15*(19), 4860.
37. Yun, J., Liu, X., Lu, Y., Guan, J., & Liu, X. (2024). DRPChain: A new blockchain-based trusted DRM scheme for image content protection. *PloS one*, *19*(9), e0309743.
38. Zhang, X., Zhang, W., Sun, W., Sun, X., & Jha, S. K. (2022). A Robust 3-D Medical Watermarking Based on Wavelet Transform for Data Protection. *Computer Systems Science & Engineering*, *41*(3).
39. Zheng, X., Lei, Q., Yao, R., Gong, Y., & Yin, Q. (2018). Image segmentation based on adaptive K-means algorithm. *EURASIP Journal on Image and Video Processing*, *2018*(1), 1-10.
40. Fatoni, F., Kurniawan, T. B., Dewi, D. A., Zakaria, M. Z., & Muhayeddin, A. M. M. (2025). Fake vs Real Image Detection Using Deep Learning Algorithm. *Journal of Applied Data Sciences*, *6*(1), 366-376.
41. Jin, H., Tang, Y., Liao, F., Du, Q., Wu, Z., Li, M., & Zheng, J. (2024). Adaptive noise-aware denoising network: Effective denoising for CT images with varying noise intensity. *Biomedical Signal Processing and Control*, *96*, 106548.
42. Luan, S., Xue, X., Ding, Y., Wei, W., & Zhu, B. (2021). Adaptive attention convolutional neural network for liver tumor segmentation. *Frontiers in Oncology*, *11*, 680807.
43. Mao, S., Wu, C., Shen, Z., Wang, Y., Wu, D., & Zhang, L. (2023). Neus-pir: Learning relightable neural surface using pre-integrated rendering. *arXiv preprint arXiv:2306.07632*.
44. Ünyılmaz, C. N., Kulavuz, B., Bakırman, T., & Bayram, B. (2024). Deep Learning Based Panchromatic2RGB Image Generation from VHR Images. *Mersin Photogrammetry Journal*, *6*(2), 87-92.
45. Liu, Z., Yuan, L., Tang, X., Uyttendaele, M., & Sun, J. (2014). Fast burst images denoising. *ACM Transactions on Graphics (TOG)*, *33*(6), 1-9.
46. Nasreen, G., Haneef, K., Tamoor, M., & Irshad, A. (2023). A comparative study of state-of-the-art skin image segmentation techniques with CNN. *Multimedia Tools and Applications*, *82*(7), 10921-10942.
47. Chai, D., Newsam, S., & Huang, J. (2020). Aerial image semantic segmentation using DCNN predicted distance maps. *ISPRS Journal of Photogrammetry and Remote Sensing*, *161*, 309-322.
48. Nie, T., Zhao, Y., & Yao, S. (2024). ELA-Net: An Efficient Lightweight Attention Network for Skin Lesion Segmentation. *Sensors*, *24*(13), 4302.